J Mater Sci (2009) 44:1780–1786
DOI 10.1007/s10853-009-3260-y

Magnetic entropy change in the monovalent doping $La_{0.7}Ba_{0.2}M_{0.1}MnO_3$ (M = Na, Ag, K) manganites

W. Cheikh-Rouhou Koubaa · M. Koubaa ·
Abdelwaheb Cheikhrouhou

Received: 4 August 2008 / Accepted: 8 January 2009 / Published online: 7 February 2009

Abstract Structural, magnetic, and magnetocaloric properties of monovalent doped $La_{0.7}Ba_{0.2}M_{0.1}MnO_3$ (M = Na, Ag, K) powder samples, synthesized using the solid state reaction at high temperature, have been experimentally investigated. The Rietveld refinement of the X-ray powder diffraction shows that all our synthesized samples are single phase and crystallize in the distorted rhombohedral system with $R\bar{3}c$ space group. Lattice parameters and the unit cell volume increases with increasing average A-site ionic radius $\langle r_A \rangle$. The Mn–O–Mn bond angle decreases with increasing $\langle r_A \rangle$, ranging from 168.32° (M = Na) to 165.91° (M = K). All our studied samples undergo a paramagnetic–ferromagnetic transition. The Curie temperature T_C, shifts slightly to a lower temperature with increasing $\langle r_A \rangle$, which is consistent with large cationic disorder. Magnetic entropy change, $|\Delta S_M|$, deduced from isothermal magnetization curves, reaches 3.04, 3.14, and 3.01 J/kg K for M = Na, Ag, and K, respectively, in a magnetic applied field change of 5T. Large relative cooling power (RCP) value of 337.9 J/kg is obtained for $La_{0.7}Ba_{0.2}K_{0.1}MnO_3$ sample, at a field change of 5T. This relatively large value associated to a Curie temperature of 311.5 K makes the present compound a promising candidate for the magnetic refrigerators around room temperature.

Introduction

Since the observation of large magnetocaloric effect (MCE) near the Curie temperature T_C in the perovskite manganite $La_{1-x}M_xMnO_3$ (M = Ca, Sr, Ba,…, etc.), there has been renewed interest in these compounds as a working substance in magnetic refrigeration technology operating at room temperature [1–4]. The origin of the MCE is based on the adiabatic demagnetization and the application of a magnetic field in a ferromagnetic material induces a spin reorientation thus decreasing the spin entropy [5]. This process is accompanied by a rise of the lattice entropy when the field is applied adiabatically. On the contrary, if we remove off the magnetic applied field, the spin system tends to randomize which increases the spin entropy, reduces the lattice one, and consequently lowers the temperature of the system. The MCE is intrinsic to the magnetic materials and can be quantified by the isothermal magnetic entropy change, $|\Delta S_M|$. The main requirements for a magnetic material to possess a large $|\Delta S_M|$, are the large spontaneous magnetization as well as the sharp drop in the magnetization associated with the ferromagnetic to paramagnetic transition at the Curie temperature T_C [6, 7].

The $La_{1-x}Ba_xMnO_3$ phase diagram shows that compositions in the range $0.2 < x < 0.5$ are ferromagnetic–metallic [8]. In this system, double exchange interactions and the localized lattice distortions, arising from Jahn–Teller effect, have been invoked to explain the magnetotransport properties [9–12]. Xu et al. [13] measured the MCE of $La_{0.67}Ba_{0.33}MnO_3$ and found that the maximum entropy change, $|\Delta S_M^{Max}|$, corresponding to a magnetic field variation, ΔH, of 2T is 1.71 J/kg K at 350 K. In order to attain large magnetic entropy changes induced by low magnetic field changes at room temperature, many researchers have shown that Curie temperature as well as

---

W. C.-R. Koubaa · M. Koubaa · A. Cheikhrouhou (✉)
Laboratoire de Physique des Matériaux, Faculté des Sciences de Sfax, B. P. 1171, 3000 Sfax, Tunisia
e-mail: abdel.cheikhrouhou@fss.rnu.tn;
abdcheikhrouhou@yahoo.fr

A. Cheikhrouhou
Institut NEEL, CNRS, B. P. 166, 38042 Grenoble Cedex9, France

magnetic entropy change can be tuned by controlling the relative ratio Mn^{3+}/Mn^{4+}, the average size of the A-cation site $\langle r_A \rangle$, and the disorder degree of the so-called mismatch A-site effect given by $\sigma^2 = \sum y_i r_i^2 - \langle r_A \rangle^2$ (y_i: fractional occupancy). Soma et al. [14] investigated the MCE properties of $La_{0.7}Ba_{0.3-x}Na_xMnO_3$ and found that with decreasing both $\langle r_A \rangle$ and σ^2, $\left|\Delta S_M^{Max}\right|$ decreases from 1.048 J/kg K ($x = 0.05$) to 0.624 J/kg K ($x = 0.15$) under $\Delta H = 0.8T$. Chen et al. [15] investigated the MCE properties of $La_{0.7-x}Nd_xBa_{0.3}MnO_3$ and found that with increasing Nd content, the T_C decreases from 333 K for $x = 0$ to 269 K for $x = 0.15$, while $\left|\Delta S_M^{Max}\right|$ increases and reaches 2.22 J/kg K upon a magnetic applied field change of 1T. Phan et al. [16] investigated the MCE properties of $La_{0.7}Ca_{0.3-x}Ba_xMnO_3$ and found that for $x = 0.12$, $\left|\Delta S_M^{Max}\right|$ reaches 1.85 J/kg K upon a magnetic applied field change of 1T. In the present work, we elaborated by the solid state method at high temperature the $La_{0.7}Ba_{0.2}M_{0.1}MnO_3$ (M = Na, Ag, and K) powder samples and investigated the effect of the monovalent substitution on the structural, magnetic, and magnetocaloric properties.

Experimental

Powder samples of $La_{0.7}Ba_{0.2}M_{0.1}MnO_3$ (M = Na, Ag, and K) have been synthesized using the standard solid state reaction method at high temperature. The starting materials were intimately mixed in an agate mortar and then heated in air up to 1000 °C for 60 h. The obtained powders were then pressed into pellets (of about 1 mm thickness and 13 mm diameter) and sintered at 1100 °C in air for 60 h with intermediate regrinding and repelling. Finally, these pellets were rapidly quenched to room temperature in air in order to freeze the structure at the annealed temperature. Phase purity, homogeneity, and cell dimensions were determined by powder X-ray diffraction at room temperature. Structural analysis was carried out using the standard Rielveld technique [17, 18]. Magnetization measurements versus temperature in the range 20–350 K and versus magnetic applied field up to 7T were carried out using a vibrating sample magnetometer. MCE were deduced from the magnetization measurements versus magnetic applied field up to 7T at several temperatures.

Results and discussion

In our studied samples, the Mn^{4+} amount remains constant equal to 40%. Monovalent element doping leads to a change in the average ionic radius $\langle r_A \rangle$ and the mismatch size σ^2 of the A-cation site. The X-ray powder diffraction (XRD) patterns at room temperature for the $La_{0.7}Ba_{0.2}M_{0.1}MnO_3$ (M = Na, Ag, and K) samples are shown in Fig. 1. The profile refinement is started with scale and background parameters followed by the unit cell parameters. Then, the peak asymmetry and preferred orientation corrections are applied. Finally, the positional parameters and the individual isotropic parameters are refined. The atomic occupations were set in terms of formula and not refined in this work. The refinements show that all our samples crystallize in the rhombohedral system with $R\overline{3}c$ space group. As expected the silver doped sample, $La_{0.7}Ba_{0.2}Ag_{0.1}MnO_3$ undergoes a mixed phase system in the rhombohedral structure composed of both manganite and residual Ag metal [19, 20]. Detailed results of the structural parameters deduced from the Rietveld analysis are listed in Table 1. In this table the average size of A-site cations ($\langle r_A \rangle$) and the mismatch size at the A-site (σ^2) are also listed. The average ionic radius has been calculated using the coordination number eight [21, 22]. With increasing $\langle r_A \rangle$, the unit cell volume increases from 355.04 Å^3 (M = Na) to 357.73 Å^3 (M = K) as shown in Table 1. It is well-known that the rhombohedral distortion results from the rotation of the MnO_6 octahedra around the [111] direction. The values of the MnO_6 octahedral tilts, determined from the oxygen positions, are 7.12°, 7.29°, and 8.58° for M = Na, Ag, and K, respectively. The lower rotation of the MnO_6 octahedra for $La_{0.7}Ba_{0.2}Na_{0.1}MnO_3$ sample is represented by larger Mn–O–Mn bond angle and the lower Mn–O bond distance as shown in Table 1. It can also be seen that the Mn–O–Mn bond angle increases with increasing $\langle r_A \rangle$, while the Mn–O bond length displays the inverse correlation to the variation in the Mn–O–Mn bond angle.

Magnetization measurements versus temperature in the range 20–350 K in a magnetic applied field of 50 mT showed that all our synthesized samples exhibit a transition from paramagnetic to ferromagnetic state with decreasing temperature (Fig. 2a). The Curie temperature T_C, determined from the position of the inflexion point in the M(T) curve, is found to be 320.5 K, 318 K, and 311.5 K for M = Na, Ag, and K, respectively. It should be noted that such method gives for T_C higher value than that obtained using the minimum of dM/dT (310.5 K, 297 K, and 268.5 K for M = Na, Ag, and K, respectively). Several researchers have confirmed that usually the Curie temperature T_C shifts to higher values with increasing $\langle r_A \rangle$ or decreasing σ^2 [23–26]. As it can be seen from Fig. 2b, T_C undergoes first a modest decrease; while with further increasing $\langle r_A \rangle$ (M = K), the mismatch effect prevails over $\langle r_A \rangle$ leading to a decrease in T_C. It should be noticed that for M = Na and Ag the ionic radius of the A-site increases slightly while the cationic disorder and the Mn^{3+}/Mn^{4+} ratio remain constant. Rivas-Padilla et al. [27] have reported the study of physical properties in manganites with fixed structural parameters ($\langle r_A \rangle = 1.23$ Å, $\sigma^2 = 0.005$ Å^2, and Mn^{3+}/Mn^{4+}=33%) and have shown that all compounds present similar Curie temperature as well as metal-insulator transition temperature.

For all our samples, in the paramagnetic phase ($T > T_C$), the temperature dependence of the magnetic susceptibility follows the Curie–Weiss law, $\chi = \frac{C}{T-\theta_P}$, where C is the Curie constant and θ_P is the Curie–Weiss temperature (inset Fig. 2a). The values of θ_P were found to be 325 K, 320 K, and 315 K for M = Na, Ag, and K, respectively. The positive θ_P values imply the ferromagnetic nature of the magnetic interactions between Mn ions. The Curie constant values calculated from the line slopes of the reciprocal susceptibility versus temperature curve, χ^{-1}(T), have been used to estimate the experimental effective paramagnetic moment $\mu_{\rm eff}^{\rm exp}$. The effective paramagnetic moment $\mu_{\rm eff}^{\rm th}$ theoretically expected can be calculated as 4.5 μ_B for all the investigated samples. The $\mu_{\rm eff}^{\rm exp}$ value is found to be 3.43 μ_B, 3.02 μ_B, and 2.74 μ_B for M = Na, Ag, and K, respectively. These values are smaller than the theoretical one, signature of a large spin-orbit coupling occurring in our compounds and resulting in a gyromagnetic factor less than 2.

In order to confirm the ferromagnetic behavior of our samples at low temperatures, we performed magnetization measurements versus magnetic applied field up to 7T at several temperatures. The magnetization evolution versus magnetic applied field for $La_{0.7}Ba_{0.2}Na_{0.1}MnO_3$ sample is plotted in Fig. 3. Below T_C, the magnetization M increases sharply with magnetic applied field for $H < 0.5$T and then saturates above 1T. The experimental value of the spontaneous magnetization $M_{\rm sp}$(exp), deduced from the $M(H)$ curves is found to be 3.36 μ_B/Mn. The magnitude of the $M_{\rm sp}$(exp) is smaller than the theoretical value of 3.6 μ_B/Mn calculated for full spin alignment. Figure 4a–c shows the Arrott plots (M^2 versus H/M) obtained from magnetization isotherms for our synthesized samples. As can be seen, Arrott plots above T_C shows a linear behavior which indicates that a second order magnetic transition occurs [28]. Figure 4d shows the temperature dependence of the spontaneous magnetization and the inverse of the susceptibility deduced from Arrott plots for $La_{0.7}Ba_{0.2}Na_{0.1}MnO_3$ sample. The estimated values of the critical exponent, associated with the spontaneous magnetization, are found to be 0.33, 0.26, and 0.21 for M = Na, Ag, and K, respectively.

The magnetic entropy change, $|\Delta S_M|$, has been calculated from isothermal magnetization measurements. Based on Maxwell's relations, $|\Delta S_M|$, can be evaluated using the following equation $|\Delta S_M| = \sum_i \frac{M_i - M_{i+1}}{T_{i+1} - T_i} \Delta H_i$ where M_i and M_{i+1} are the experimental values of magnetization measured at temperatures T_i and T_{i+1}, respectively, under

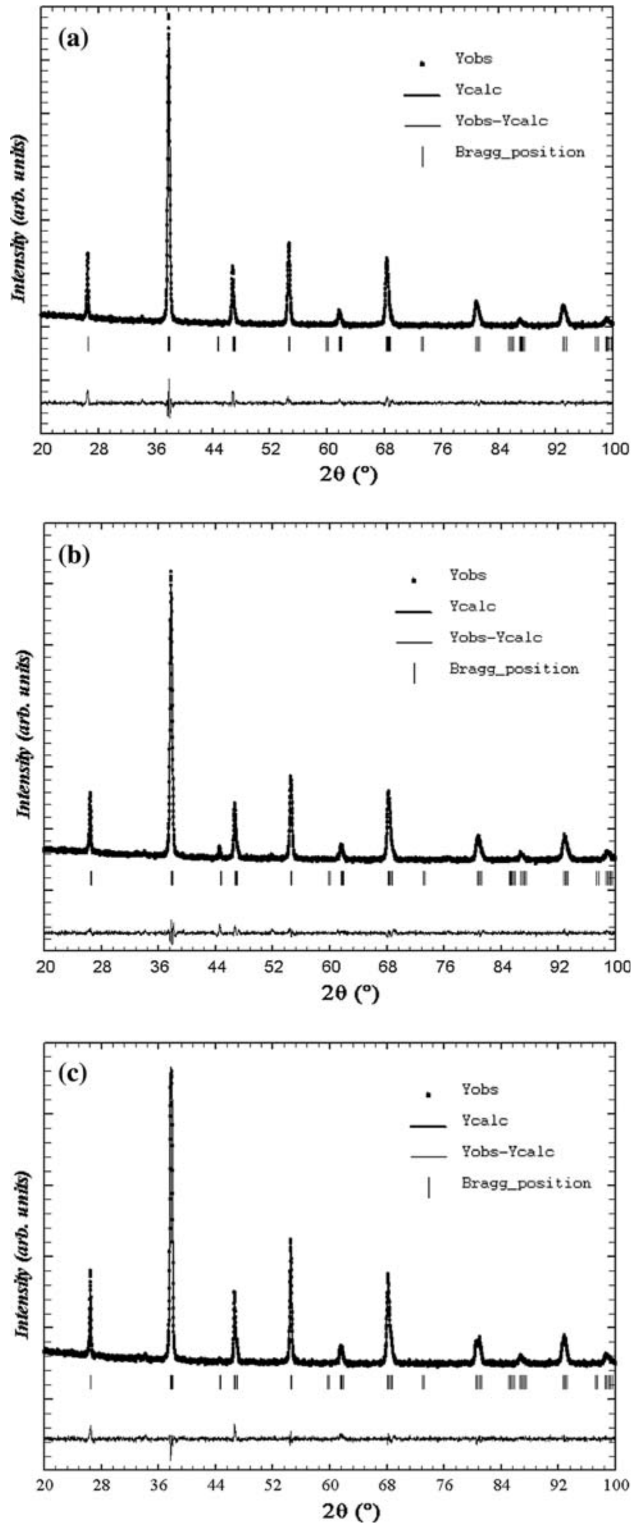

Fig. 1 XRD patterns of $La_{0.7}Ba_{0.2}M_{0.1}MnO_3$ compounds. **a** M = Na, **b** M = Ag, and **c** M = K. Squares indicate the experimental data and the calculated data is the continuous line overlapping them. The lowest curve shows the difference between experimental and calculated patterns. The vertical bars indicate the expected reflection positions

Table 1 Refined structural parameters of $La_{0.7}Ba_{0.2}M_{0.1}MnO_3$ samples (M = Na, Ag, and K) at room temperature

	$La_{0.7}Ba_{0.2}Na_{0.1}MnO_3$	$La_{0.7}Ba_{0.2}Ag_{0.1}MnO_3$	$La_{0.7}Ba_{0.2}K_{0.1}MnO_3$
a(Å)	5.520(8)	5.531(1)	5.538(6)
b(Å)	5.520(8)	5.531(1)	5.538(6)
c(Å)	13.450(7)	13.465(6)	13.466(1)
V(Å^3)	355.04(3)	356.75(1)	357.73(6)
Mn–O(Å)	1.959(7)	1.962(8)	1.968(6)
Mn–O–Mn(°)	168.32(4)	168.06(5)	165.91(4)
$\langle r_A \rangle$(Å)	1.214	1.224	1.247
σ^2(Å^2)	10.64×10^{-3}	10.86×10^{-3}	18.20×10^{-3}
χ^2	1.42	1.17	1.15

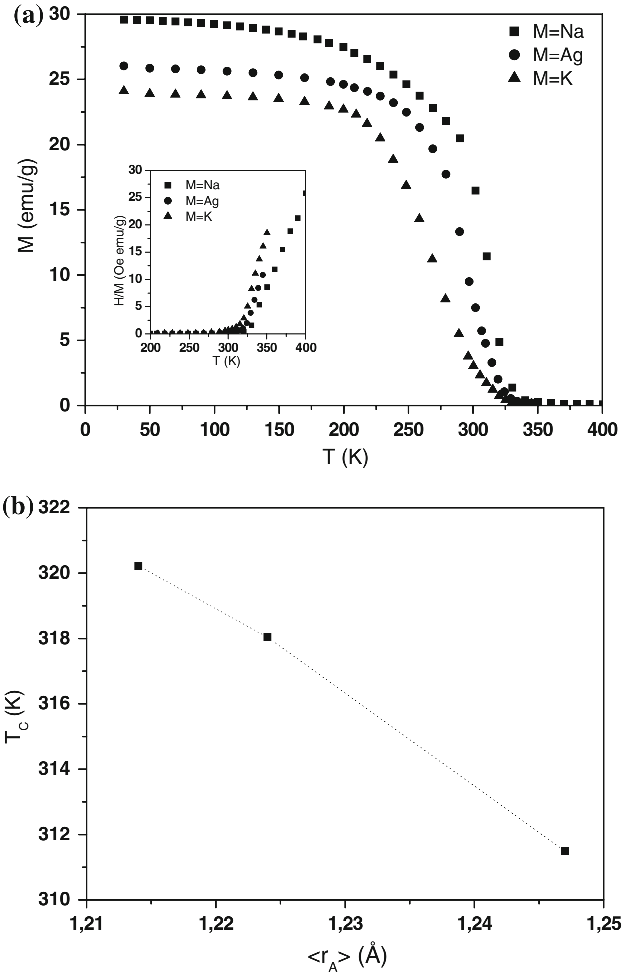

Fig. 2 **a** Temperature dependence of the magnetization at μ_0H = 50 mT (the inset shows the temperature dependence of reciprocal magnetic susceptibility) and **b** Curie temperature evolution versus $\langle r_A \rangle$ for $La_{0.7}Ba_{0.2}M_{0.1}MnO_3$ samples

magnetic applied field H_i [29]. Figure 5a–c shows $|\Delta S_M|$ of the $La_{0.7}Ba_{0.2}M_{0.1}MnO_3$ (M = Na, Ag, and K) samples as a function of temperature for several external magnetic field. All our samples exhibit large MCE effect around the magnetic transition temperature and the magnitude of $|\Delta S_M|$ increases with increasing the magnetic applied field. Our samples exhibit a maximum entropy change, $|\Delta S_M^{Max}|$, equal to 0.77 J kg^{-1} K^{-1}, 0.71 J kg^{-1} K^{-1}, and 0.74J kg^{-1} K^{-1} upon a magnetic field change of 1T and 3.87 J kg^{-1} K^{-1}, 3.85 J kg^{-1} K^{-1}, and 3.97 J kg^{-1} K^{-1} upon 7T, respectively for M = Na, Ag, and K. For $La_{0.7}Ba_{0.2}Na_{0.1}MnO_3$ specimen, the evolution of $|\Delta S_M|$ as a function of temperature shows two sharp peaks with $|\Delta S_M^{Max}|$ values of 3.16 J/kg K and 3.87 J/kg K upon a magnetic field change of 7T. The second maximum occurs, as expected, at the magnetic transition temperature. The relative cooling power (RCP) is evaluated as $RCP = -\Delta S_M(T,H) \times \delta T_{FWHM}$ where δT_{FWHM} is the full-width at half-maximum of $|\Delta S_M|$ versus temperature [30]. For our samples, the RCP value is found to be 307.1 J/kg, 271 J/kg, and 337.9 J/kg at 5T for M = Na, Ag, and K, respectively. The RCP value of $La_{0.7}Ba_{0.2}K_{0.1}MnO_3$ sample is higher in magnitude and occurs close to room temperature compared to M = Na and Ag samples. In addition the magnitude of the RCP is about 82% of that of pure Gd [6]. Phan et al. [31] reported an overview on magnetocaloric properties of manganite

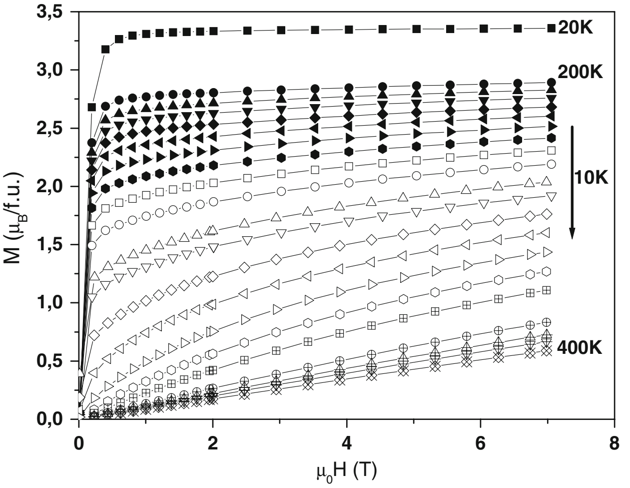

Fig. 3 Magnetization evolution versus magnetic applied field at several temperatures for $La_{0.7}Ba_{0.2}Na_{0.1}MnO_3$ sample

Fig. 4 M^2 versus H/M isotherms for $La_{0.7}Ba_{0.2}M_{0.1}MnO_3$ samples **a** M = Na, **b** M = Ag, **c** M = K and **d** The spontaneous magnetization (M_{sp}) and inverse of susceptibility $1/\chi$ as a function of temperature for $La_{0.7}Ba_{0.2}Na_{0.1}MnO_3$ compound

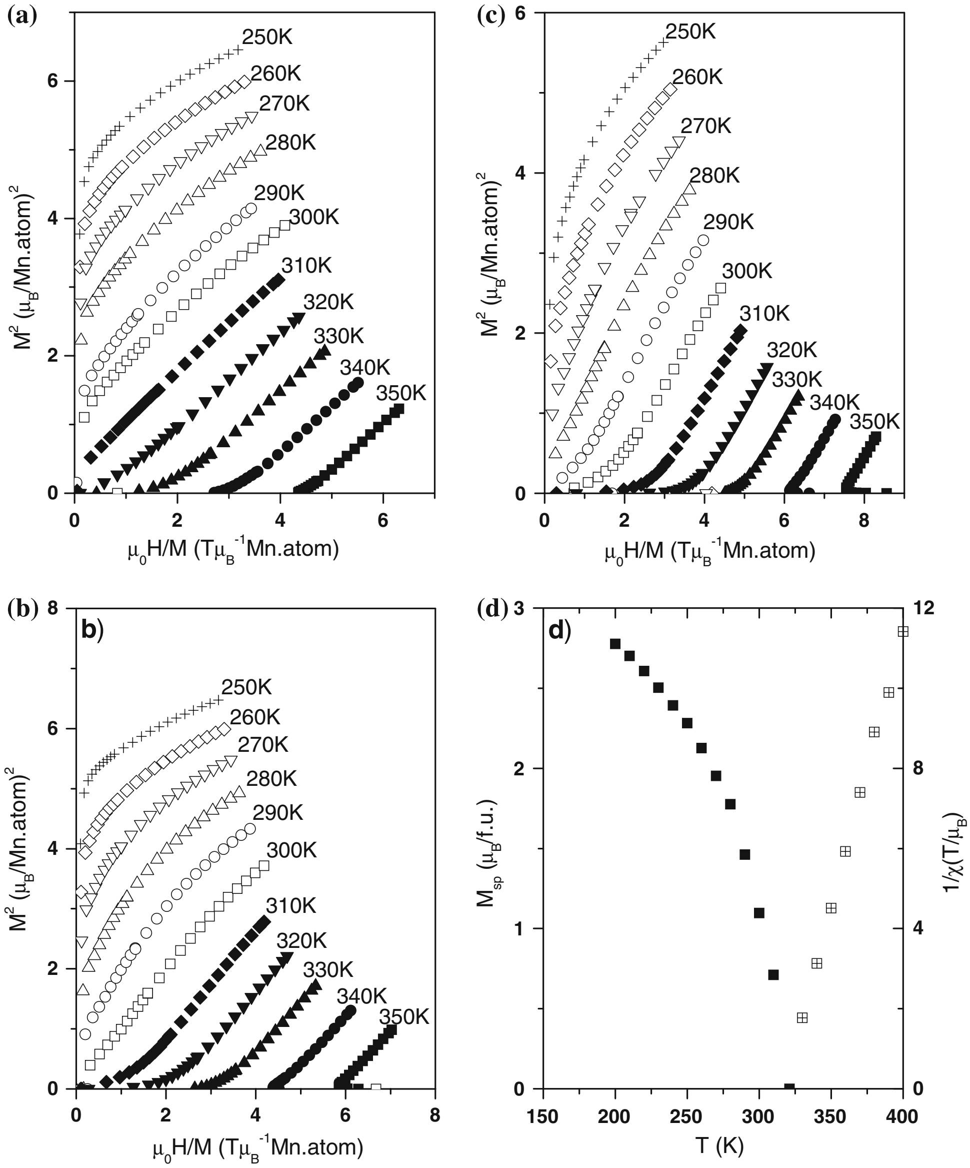

materials. The higher RCP value is observed in $La_{0.845}Sr_{0.155}MnO_3$ [31] which reaches 670 J/kg under 7T around 235 K making difficult its application in magnetic refrigeration near room temperature. Moreover, $La_{0.7}Ca_{0.25}Sr_{0.05}MnO_3$ [32] and $La_{0.7}Ca_{0.2}Sr_{0.1}MnO_3$ [7] compounds are, respectively, characterized by an RCP value of 462 J/kg (5T) and 374 J/kg (5T) around room temperature which are comparable to our results. In order to further quantify the efficiency of our synthesized samples as a refrigerant, the heat originated only from magnetic entropy change can be calculated using the relation $\left|Q_{\mathrm{M}}(T, 1\mathrm{T}) = \int_{T_{\mathrm{C}}-\Delta T}^{T_{\mathrm{C}}+\Delta T} |\Delta S_{\mathrm{M}}(T, 1\mathrm{T})|\right|$. The temperature range, ΔT, for which $\Delta S_{\mathrm{M}}/\Delta S_{\mathrm{M}}^{\mathrm{Max}} > 75\%$, is found to be 44 K, 40 K, and 49 K for M = Na, Ag, and K, respectively. A typical curve $\Delta S_{\mathrm{M}}/\Delta S_{\mathrm{M}}^{\mathrm{Max}}$ versus temperature is plotted in Fig. 5d for M = K. These wide temperature values associated to large magnetic entropy change is very beneficent for an ideal Ericsson refrigeration cycle [33]. The Q_{M} values are determined to be 40.3 J/kg, 44.5 J/kg, and 49.4 J/kg for M = Na, Ag, and K, respectively. Our results may be interesting enough, compared to materials considered as good for applications in magnetic refrigerators, opening a way for investigations of materials useful for magnetic refrigeration.

Conclusions

We investigated the effect of monovalent doping on the physical properties of $La_{0.7}Ba_{0.2}M_{0.1}MnO_3$ (M = Na, Ag, and K) powder samples. The structural study shows that all our synthesized compounds crystallize in the rhombohedral

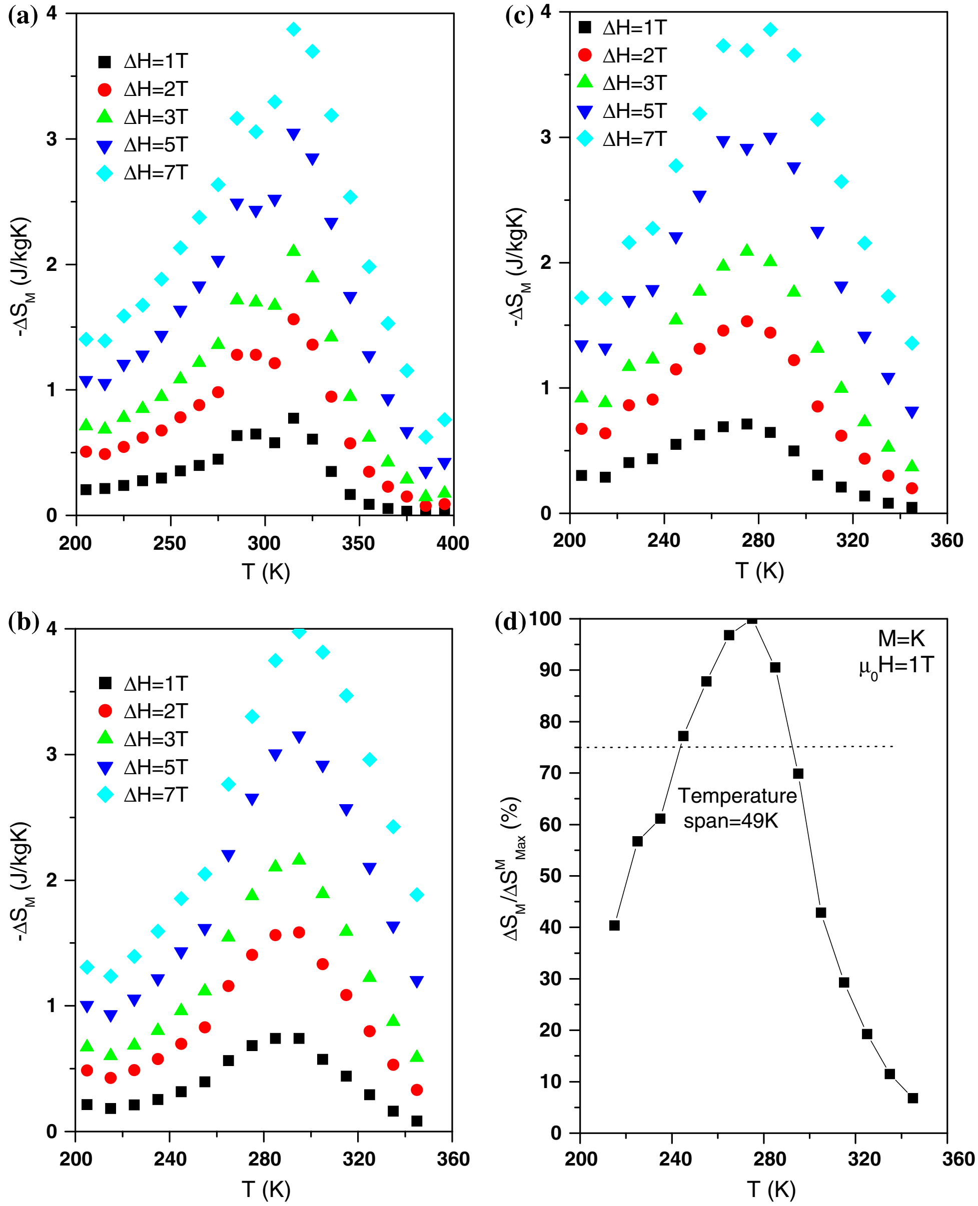

Fig. 5 Magnetic entropy change $|\Delta S_M|$ as a function of temperature at several magnetic applied field for $La_{0.7}Ba_{0.2}M_{0.1}MnO_3$ samples, **a** M = Na, **b** M = Ag, **c** M = K, and **d** Typical plot showing $\Delta S_M/\Delta S_M^{Max}$ versus temperature for M = K sample

structure with $R\bar{3}c$ space group. All our samples exhibit a paramagnetic–ferromagnetic transition with decreasing temperature. A large MCE is observed in our samples. $La_{0.7}Ba_{0.2}K_{0.1}MnO_3$ sample exhibits the highest RCP value of 337.9 J/kg upon a magnetic applied field change of 5T.

Acknowledgements This study has been supported by the Tunisian Ministry of Higher Education, Scientific Research and Technology.

References

1. Guo ZB, Zhang JR, Huang H, Ding WP, Du YW (1997) Appl Phys Lett 70:904
2. Guo ZB, Du YW, Zhu JS, Huang H, Ding WP, Feng D (1997) Phys Rev Lett 78:1142
3. Phan MH, Phan TL, Yu SC, Tho ND, Chau N (2004) Phys Status Solid B 241:1744
4. Gschneidner KA Jr, Pecharsky VK, Tsokol AO (2005) Rep Prog Phys 68:1479
5. Werbung E (1881) Ann Phys Chem 13:141
6. Dan'kov SY, Tishin AM, Pecharsky VK, Gschneidner KA (1998) Phys Rev B 57:3478
7. Phan MH, Yu SC, Hur NH (2005) Appl Phys Lett 86:072504
8. Ju HL, Nam YS, Lee JE, Shin HS (2000) J Magn Magn Mater 219:1
9. Zener C (1951) Phys Rev 82:403
10. Millis AJ, Littlewood PB, Shraiman BI (1995) Phys Rev Lett 74:5144
11. Roder H, Zang J, Bishop AP (1996) Phys Rev Lett 76:1356
12. Dagotto E, Hotta T, Moreo A (2001) Phys Rep 344:1
13. Xu Y, Meier M, Das P, Koblischka MR, Hartmann U (2002) Cryst Eng 5:383
14. Das S, Dey TK (2008) Mater Chem Phys 108:220

15. Chen W, Nie LY, Zhong W, Shi YJ, Hu JJ, Li AJ, Du YW (2005) J Alloy Compd 395:23
16. Phan MH, Tian SB, Yu SC, Ulyanov AN (2003) J Magn Magn Mater 256:306
17. Rietveld HM (1969) J Appl Cryst 2:65
18. Rodriguez-Carvajal J (1990) A program for rietveld refinement and pattern matching analysis (Satellite meeting on powder diffraction of the XV IUCr congress), p 127
19. Ye SL, Sang WH, Dai JM, Wang KY, Wang SG, Zhang CL, Du JJ, Sun YP, Fang J (2002) J Magn Magn Mater 248:2633
20. Pal S, Banerjee A, Choudhuri BK (2003) J Phys Chem Solids 64:2063
21. Shannon RD (1976) Acta Crystallogr A32:751
22. Pi L, Hervieu M, Maignan A, Martin C, Raveau B (2003) Solid State Commun 126:229
23. Rodriguez-Martinez LM, Paul Attfield J (1996) Phys Rev B 54:R15622
24. Rodriguez-Martinez LM, Paul Attfield J (1998) Phys Rev B 58:242
25. Terai T, Kakeshita T, Fukuda T, Saburi T, Takamoto N, Kindo K, Honda M (1998) Phys Rev B 58:14908
26. Vanitha PV, Santhosh PN, Singh RS, Rao CNR, Attfield JP (1999) Phys Rev B 59:13539
27. Rivas-Padilla EP, Lisboa-Filho PN, Ortiz WA (2004) J Solid State Chem 177:1338
28. Singh NK, Suresh KG, Nigam AK (2003) Solid State Commun 127:373
29. McMichael RD, Ritter JJ, Shull RD (1993) J Appl Phys 73:6946
30. Gschneidner KA, Pecharsky VK (2000) Annu Rev Mater Sci 30:387
31. Phan MH, Yu SC (2007) J Magn Magn Mater 308:325
32. Szewczyk A, Gutowska M, Dabrowski B, Plackowski T, Danilova NP, Gaidukov YP (2005) Phys Rev B 71:224432
33. Hasimoto T, Kuzuhara T, Sahashi M, Inomata K, Tomokiyo A, Yayama H (1987) J Appl Phys 62:3873